Hot Dry Rocks Pty Ltd
Geothermal Energy Consultants

HEAD OFFICE
PO Box 251
South Yarra, Vic 3141
Australia
T +61 3 9827 7740
E info@hotdryrocks.com
W www.hotdryrocks.com

ABN: 12 114 617 622

SERVICES
Exploration
Rock Property Measurements
Project Development
Portfolio Management
Grant Applications

Fault Stress State Modelling of Potential Fault Plays, Charleton-Lemont Project, Tasmania.

Prepared for KUTh Energy Ltd

28 October 2010

Executive Summary

Hot Dry Rocks Pty Ltd was commissioned by KUTh Energy Ltd to complete preliminary numerical fault stress state modelling at its Charleton-Lemont prospect (SEL26/2005), Tasmania. The purposes of this modelling exercise are:

1. To provide estimates of the potential stress state of all interpreted major fault structures within the selected area.
2. To identify "critically stressed" faults and/or fault segments and by corollary their potential to contain zones of enhanced permeability i.e. potential Fault Play targets.
3. To reduce the risk and uncertainty of exploring for fault-related geothermal targets.

From one local *in situ* stress measurement and a limited amount of regional *in situ* stress datasets it is interpreted that the Charleton-Lemont prospect is under the influence of an ~E–W oriented thrust fault stress regime. This apparent thrust fault stress regime is optimal for EGS developments as hydraulic stimulation is expected to result in approximately horizontal fracture/reservoir growth. An ~E–W maximum horizontal stress (S_H) orientation indicates that 'critically stressed' fractures/faults would be either steeply dipping ~NE–SE trending structures or shallow (<45°) dipping structures such as shallow thrust and back splay faults observed in the regional cross- and long-sections. Estimates of local stress magnitude data indicate a differential stress regime (i.e. S_H, S_h and S_V) of approximately 2 : 1.5 : 1.

The modelling results for both the regional cross- and long-section indicate that shallow to moderate dipping faults are potentially critically stressed consistent with predictions based on the theory of stress-dependent fracture permeability. These shallow to moderate dipping fault structures should be considered as favourable Fault Play targets. Both versions of the 5000 m depth horizontal planar models identified two fault intersections that appear to be critically stressed and potentially zones of enhanced permeability. These two sites involve the intersection of ~N–S and ~NW–SE faults hosted within metasediments in close proximity to a major granite contact. Of those two sites the southern fault intersection appears to have a more prominent stress field anomaly and ranks higher as a potential permeable fault

intersection. The model results of both versions of the 2000 m depth horizontal planar models found little to no evidence of critically stressed faults or localised stress field anomalies.

Critically stressed faults are exploration targets if they represent zones of enhanced fault-associated permeability. However, it is important to note that the large model parameter uncertainties mean that the modelling results are preliminary indications only i.e. a ‘probabilistic’ representation of potential fault stress states. Other natural processes may produce a counter effect.

Table of Contents

Authors

Luke Mortimer compiled this report. Gareth Cooper reviewed the report.

Copyright

Disclaimer

1. Introduction

Hot Dry Rocks Pty Ltd (HDR) has prepared this report for KUTh Energy Ltd (KEN) to document the results of preliminary fault stress state modelling at its Charleton-Lemont prospect (SEL26/2005), Tasmania. Namely, to investigate through numerical modelling the stress state and potential permeability of the major fault structures within the prospect (Figure 1).

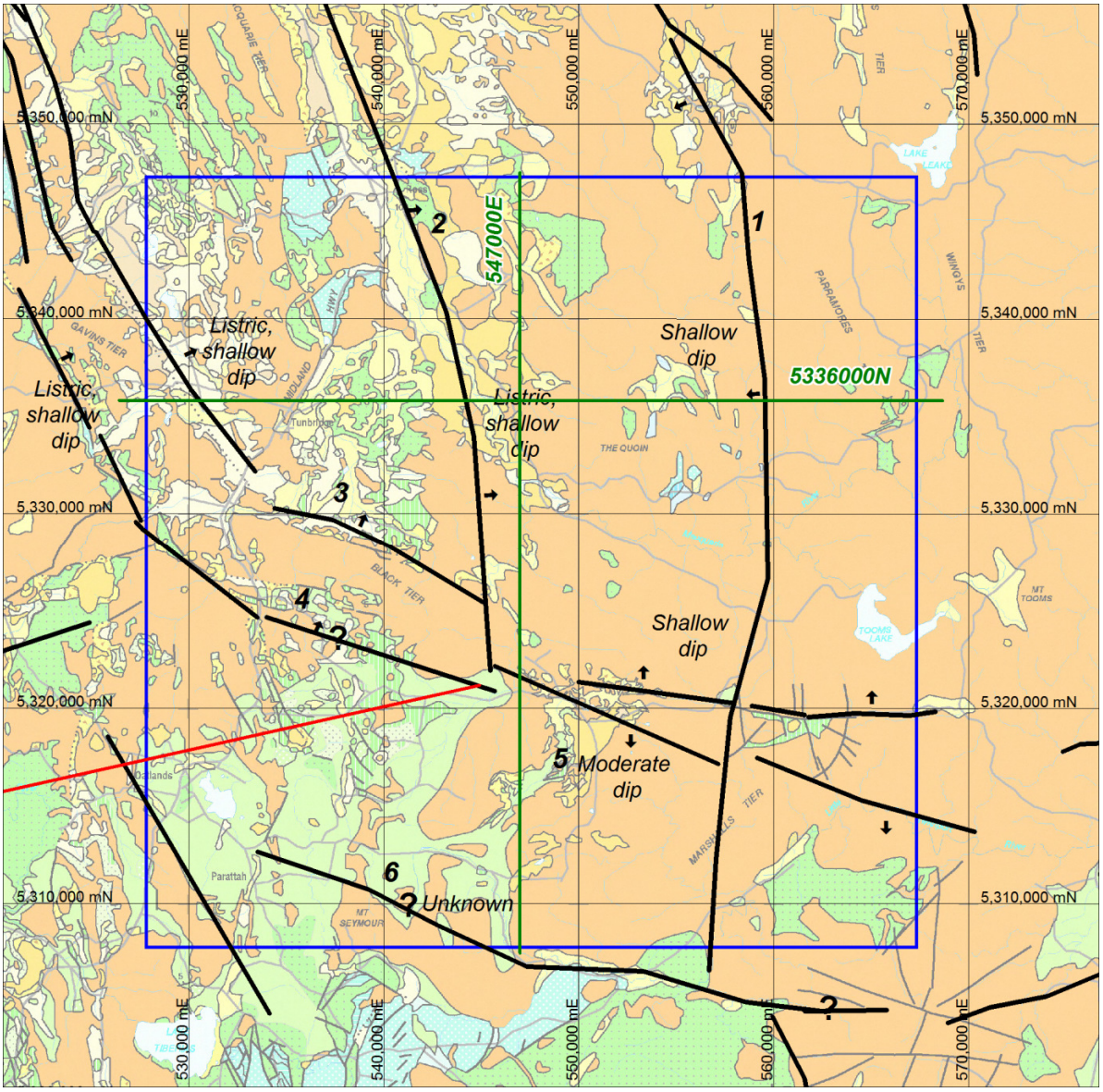

Figure 1. *Fault interpretation map (at surface) of the Charleton-Lemont Geothermal Play on a background surface geology image (provided by KEN). Major faults and their dip directions denoted by black lines and arrows. Red line denotes an inferred fault. Horizontal planar model extents = blue outline (see Sections 4.1 to 4.4). Location of regional cross- and long-section = green lines (see Sections 4.5 and 4.6).*

Permeable fault structures present an attractive geothermal exploration target as they have been proven to substantially boost overall reservoir permeability and fluid production at some existing geothermal energy operations (e.g. Dixie Valley, USA; Landau, Germany). However, not all faults are permeable. Their hydraulic properties are inherently heterogeneous and difficult to characterize, making it challenging to distinguish between faults acting as fluid conduits or fluid barriers. This challenge is compounded when a fault no surface expression because to achieve sufficiently high production fluid temperatures a fault typically must be intersected at a significant depth (>2 km) where the exact hydraulic nature of the fault is unknown prior to drilling. Therefore, when exploring for permeable fault targets HDR recommends fault stress state modelling to identify zones of potentially enhanced permeability at the inferred target depth and under the *in situ* stress field conditions.

The numerical modelling in this report utilised the 'Universal Distinct Element Code' (UDEC™)[1] which is a 2D discontinuum or discrete fracture network code that combines rock, fracture and fluid property data with the 3D *in situ* stress field to interpolate the hydro-mechanical interaction between a deformable rock mass and its fractures. Fault structures are explicitly incorporated in the models whilst the rock mass is treated as impermeable, which allows for a fully coupled hydro-mechanical analysis of a fault system. The main aims of this modelling exercise are:

1. To provide estimates of the potential stress state of all interpreted major fault structures within the model area.
2. To identify "critically stressed" faults and/or fault segments and by corollary their potential to contain zones of enhanced permeability i.e. potential Fault Play targets.
3. To reduce the risk and uncertainty of exploring for fault-related geothermal targets.

For the purposes of this modelling exercise, KEN provided several geological interpretations of the Charleton-Lemont Project for use in the construction of the UDEC™ models. KEN also provided local stress regime data. An independent review of this data was not conducted by HDR as part of this study. Other model parameters in-

[1] UDEC™ is a product of the Itasca Consulting Group, Minneapolis, USA.

cluding rock mass and fault properties (e.g. rock density, bulk moduli, fault stiffness etc) were defined by HDR based on published values and empirical relationships. As no rock mass or fault property data have been sampled or measured these model parameters are all inferred. Therefore, all model results should be considered preliminary and stochastic in nature only. All results and conclusions of this modelling exercise are based purely on an assessment of the modelled stress fields as shown in the figures contained at the end of this report. Full fluid flow modelling and analysis was not considered warranted given the preliminary stochastic nature of these models plus the significant computational time that these would require.

2. Fault Plays

Targeting fault structures involves exploring at depth for zones of enhanced natural *in situ* fracture porosity and permeability to maximise geothermal fluid production from a prospective area. A permeable fault target can be viewed as either: (1) having sufficient natural *in situ* porosity and permeability with natural fluid recharge occurring at the optimal fluid temperature (e.g. Dixie Valley, USA); or (2) having some enhanced porosity and permeability that may still require some degree of reservoir stimulation (e.g. Landau, Germany).

Two critical elements considered positive for fault permeability targets are:

(1) Favourable fault orientation with respect to the *in situ* stress field (i.e. 'critically stressed'); and

(2) Hydraulic contact with a significant volume of porous and/or fractured and permeable reservoir (i.e. fluid mass storage).

For the latter, the fluid mass storage may be provided by the fault structure itself or an adjoining and hydraulically connected rock unit such as thick, porous sandstone. Fluid overpressures associated with the fault may also be beneficial for fluid advection along the structure from a connected, deeper and potentially hotter reservoir and for lowering the effective stress state of the fault.

One key aspect of exploring for permeable faults is the theory of stress-dependant fracture permeability in deep-seated, fractured rocks. This theory is supported by

studies relating to hydrocarbon and geothermal reservoirs and studies of potential nuclear waste repository sites (e.g. Gentier *et al.*, 2000; Hillis *et al.*, 1997; Hudson *et al.*, 2005). The theory is that *in situ* stress fields exert a significant control on fluid flow patterns in fractured rocks, particularly, for rocks of low matrix permeability. For example, in a key study of deep (>1.7 km) boreholes, Barton et al. (1995) found that permeability manifests itself as fluid flow focused along fractures favourably aligned within the *in situ* stress field, and that if fractures are critically stressed this can impart a significant anisotropy to the permeability of a fractured rock mass. Critically stressed fractures are defined as fractures that are close to frictional failure within the *in situ* stress field (Barton *et al.*, 1995). Specifically, the theory of stress-dependent fracture permeability predicts preferential flow occurring along fractures that are oriented orthogonal to the minimum principal stress (S_3) direction (due to low normal stress), or inclined ~30° to the maximum principal stress (S_1) direction (due to shear dilation).

Critically stressed faults are exploration targets if they represent zones of enhanced fault-associated permeability. However, it is important to note that, modelling results only indicate the probability of encountering enhanced permeability. Other natural processes may produce a counter effect.

The risks of targeting permeable faults as geothermal reservoirs include: (1) a relatively high permeability structure may result in fluid pathway short-circuiting (i.e. rapid flow-through of re-injected cooler fluid and excessive reservoir thermal drawdown); (2) multiple fault structures with varying amounts of displacement may truncate and compartmentalise an aquifer (i.e. reduction in accessible reservoir volume and mass storage); and (3) the targeted fault structure may still be hydraulically sealed and/or stress-insensitive from the effects of fault mineralisation, gouge etc. These risks can be partially mitigated through interpretation of good quality reflection seismic data interpretation and with well hydraulic test data. The results of the numerical models are, however, only as accurate as the input data. The quality of stochastic rock mass models is wholly dependent on the quality of the raw input datasets.

3. Model Design and Construction

3.1. Model dimensions

The dimensions of the horizontal planar models cover an area of 39 km x 39 km (28000 mE to 67000 mE, 8000 mN to 47000 mN). The regional cross- and long-sections are defined by an area of 39 km long (0–39000 m, W–E) and 6.4 km depth (surface at 6400 m, base at 0 km).

3.2. In Situ Stress Fields

The description of any *in situ* stress field includes the relative arrangement of the three mutually orthogonal principal axes of stress referred to as the maximum (S_1), intermediate (S_2) and minimum (S_3) principal axes of stress. As the Earth's surface is a free surface with zero shear stress the vertical stress (S_V) is assumed to be one of these principal axes of stress. The other two principal axes of stress consist of the two mutually orthogonal, horizontal stress orientations referred to as the maximum and minimum horizontal principal axes of stress (S_H and S_h, respectively). In practice, far-field crustal stress regimes are classified using the Andersonian scheme, which relates the three major styles of faulting in the crust to the three major arrangements of the principal axes of stress (Anderson, 1951). These three major stress regimes are:

(a) Normal faulting stress regime where $S_V > S_H > S_h$;

(b) Strike-slip faulting stress regime where $S_H > S_V > S_h$; and

(c) Thrust (reverse) faulting stress regime where $S_H > S_h > S_V$.

To estimate the effective stress state (S') also requires that an estimate of the pore fluid pressures (P_p) within the rock formation, as S' is defined as the difference between the applied stress (S) and the internal pore fluid pressure:

$$S' = S - P_p$$

The effective stress is critical as it controls coupled hydro-mechanical behaviour (or poroelasticity) by affecting fracture deformation processes as fluid pressures act to

reduce the stress acting normal to a fracture plane. For example, high effective stresses with relatively low fluid pressures act to close fractures whilst low effective stresses with relatively high fluid pressures act to dilate fractures.

3.3. Contemporary Regional Stress Field

Currently, there is a general lack of *in situ* stress field data in Tasmania. However, a recent focal mechanism analysis of an earthquake proximal to the Charleton-Lemont prospect area ("Midlands event", 2009) provided by KEN revealed an approximately E–W oriented thrust fault stress regime (i.e. $S_H > S_h > S_v$). In addition to earthquake records, other possible evidence cited for contemporary seismic activity includes Late Quaternary reactivation of large fault structures in SW Tasmania. For example, the Lake Edgar Fault in SW Tasmania has been interpreted as an originally Cambrian-age fault that was been reactivated several times since the Late Quaternary-Holocene period (McCue *et al.*, 2003). In particular, the Lake Edgar Fault is an approximately north-trending, westerly dipping fault that has experienced recent reverse-style movement and vertical displacement suggesting that it is under the influence of approximately east-west horizontal compression (McCue *et al.*, 2003).

Currently there are no local stress magnitude data. However, the closest measured magnitude data located in the Otway and Gippsland Basins revealed differential stress magnitude ratios (i.e. $S_1 : S_2 : S_3$) approximately of the order 2 : 1.3 : 1 (Nelson *et al.*, 2006). Local Tasmanian mine and hydropower stress data suggest a ratio of approximately 2 : 1.5 : 1 (Fiona Holgate, *pers. comm.*).

For the Charleton-Lemont UDEC™ models the applied *in situ* stress field was an E–W oriented, thrust fault stress regime with stress magnitudes based upon an estimate of S_V (i.e. ρ.g.h) and applied as a differential stress ratio of 2 : 1.5 : 1.

3.4. Rock Mass and Fault Parameters

The geological interpretations provided by KEN included four broad geological formations which were described as follows:

1. Jurassic Dolerite - Generally assumed to be a flat-lying intrusive sill around 300m thick and present at surface in most places. Classic, hard, massive medium-grained dolerite. The likely presence of feeders etc. at depth has been ignored.

2. Permo-Triassic Sediment of the Tasmania Basin (Parmeener Supergroup). Generally assumed to be flat-lying bedded terrestrial and marine sediments around 1000m thick. Undeformed, unaltered, typically mudstone/siltstone/sandstone. Some coal sequences and basal tillite. This unit is defined as a "siltstone" in the UDEC™ models.
3. Metasediment, likely to comprise two units, Ordovician – Devonian (Mathinna Supergroup) or Precambrian. Present at depth between Parmeener and granite. Likely to be rheologically similar regardless of age as both groups are composed of turbidite material (sand/silt/mud) with discernable bedding but multiply deformed, folded, cleaved with veining and faults. Low grade sub- to greenschist-facies metamorphism. This unit is defined as a "phyllite" in the UDEC™ models.
4. Devonian Granite. Massive granite/granodiorite.

Rock mass properties assigned to these four units in the Charleton-Lemont UDEC™ models were sourced from the RocData[2] rock property database and Sloane (1991).

The most difficult part of this process is assigning fault stiffness values, particularly, as they are expected to vary with host lithology. As fracture stiffness is a function of wall contact area, fault normal stiffness (jkn) for smooth planar surfaces can approximate the value of the rock mass Young's Modulus (*E*) whereas fault shear stiffness (jks), for perfectly matching rough surfaces, can approximate the value of the rock mass Shear Modulus (*G*). However, prior to drill testing the true nature of the fault at depth is unknown. As the aim is to attempt to evaluate relative fault stress states, across multiple faults and lithologies, a constant low fault stiffness for each respective lithology was inferred with zero tensile strength, cohesion and dilation angle values. In theory, these geomechanical properties replicate the behaviour of a 'weak' fault plane, which allows each fault segment to potentially deform. This is a reasonable approach as most active fault zones are inferred to be weak (Gudmundsson *et al.* 2001; Gudmundsson *et al.* 2009). The use of a constant low fault stiffness is intended to differentiate fault behaviour occurring within different rock units.

No fluid pressure data is available for the Charleton-Lemont region. Therefore, fluid pressures were assumed hydrostatic commencing from the surface.

[2] RocData is a product of RocScience Inc.,Ontario, Canada.

For this modelling exercise, an elastic-isotropic rock mass constitutive model was employed whilst fracture behaviour was defined by the Coulomb-slip failure criteria. The assigned Charleton-Lemont UDEC™ model parameters are summarised in Table 1.

Table 1 Charleton-Lemont UDEC™ rock and fault model parameters.

Model Parameters	Dolerite	Siltstone	Phyllite	Granite	Units
Rock Material Density (ρ)	2900	2700	2700	2600	$kg.m^{-3}$
Poisson's Ratio (ν)	0.3	0.17	0.19	0.25	-
Young's Modulus (*E*)	100e6	27e6	52e6	154e6	Pa
Bulk Modulus (*K*)	83.3e6	13.6e6	27.9e6	102.6e6	Pa
Shear Modulus (*G*)	38.5e6	11.5e6	21.8e6	61.6e6	Pa
Fault Normal Stiffness (jk_n)	1e9	1e9	1e9	1e9	$Pa.m^{-1}$
Fault Shear Stiffness (jk_s)	1e9	1e9	1e9	1e9	$Pa.m^{-1}$
Fault Cohesion	0	0	0	0	Pa
Fault Tensile Strength	0	0	0	0	Pa
Fault Friction Angle	30	30	30	30	Degrees
Fault Dilation	0	0	0	0	Degrees
Fault Aperture (at zero stress)	0.25	0.25	0.25	0.25	mm
Fault Residual Aperture	0.01	0.01	0.01	0.01	mm
Fluid Pressure	Hydrostatic	Hydrostatic	Hydrostatic	Hydrostatic	Pa
Water Density	1000	1000	1000	1000	$kg.m^{-3}$

4. Results

The model results are described in largely qualitative terms through an analysis of the steady-state stress fields. All results referred to in this report are depicted by representative figures contained at the end of this report. Please note that these figures show a number of small stress anomalies located along model boundaries which should be ignored as these are simply artefacts of the model boundary conditions.

4.1. 2000 m depth horizontal planar model – version 1

Figures 2–4 show representative plots of the model design and the S_H and S_V stress magnitude contours, respectively. The overall results of this particular model show fairly uniform stress across the entire model and all fault structures with no discernible stress field anomalies.

4.2. 2000 m depth horizontal planar model – version 2

Figures 5–7 show representative plots of the model design and the S_H and S_V stress magnitude contours, respectively. The version 2 model differs from version 1 by the inclusion of the inferred ~ENE-WSW trending fault in the SW portion of the model area (i.e. the red coloured fault of Figure 1). The overall results of this particular model show fairly uniform stress across the entire model and all fault structures with no discernible stress field anomalies. This version 2 model was re-run with fault stiffness values lowered by an order of magnitude. However, this model re-run also did not produce any significant stress anomalies with the exception of one subtle stress (low) anomaly associated with the intersection between a ~N–S and ~ESE–WNW trending faults (Figure 6).

4.3. 5000 m depth horizontal planar model – version 1

Figures 8–10 show representative plots of the model design and the S_H and $S_{H,h}$ (i.e. horizontal shear) stress magnitude contours, respectively. The results show two distinct stress (low) anomalies associated with two fault intersections (Figures 9 and 10). These stress anomalies are restricted to the horizontal planes as they do not appear within the vertical stress field. Of these two anomalies the southernmost anomaly appears as a very distinct $S_{H,h}$ (horizontal shear) stress anomaly indicating

that this particular fault intersection is critically stressed and potentially a zone of enhanced permeability (Figure 10).

4.4. 5000 m depth horizontal planar model – version 2

Figures 11–13 show representative plots of the model design and the S_H and $S_{H,h}$ (i.e. horizontal shear) stress magnitude contours, respectively. The version 2 model differs from version 1 by the inclusion of the inferred ~ENE-WSW trending fault which transects across the entire central part of the model (i.e. the red coloured fault of Figure 1). The results show two distinct stress (low) anomalies associated with the same two fault intersections as that observed in model version 1 (Figures 12 and 13). The version 2 model results differ slightly in that these two stress anomalies appear in all stress tensor plots (i.e. S_H, S_h and S_V). Again, of these two anomalies the southern anomaly appears as a very distinct $S_{H,h}$ (horizontal shear) stress anomaly indicating that this particular fault intersection is critically stressed and potentially a zone of enhanced permeability (Figure 13). It is likely that the additional intersection by the inferred ~ENE-WSW trending fault in this version 2 model has accentuated the local stress field perturbation at this location.

4.5. Regional cross-section at 5336000 mN

Figures 14–17 show representative plots of the model design, regional S_V pattern and two small-scale examples of the stress patterns associated with the western and eastern zone faults, respectively. For all three stress tensors (i.e. S_H, S_h and S_V) shallow to moderate east- and west-dipping faults display stress perturbations along their fault planes suggesting that these faults are critically stressed and potentially zones of enhanced permeability (Figures 16 and 17). These anomalies are not observed associated with sub-horizontal faults. This pattern is expected under the imposed thrust fault stress conditions and its relatively high magnitude of E–W oriented compression (S_H).

4.6. Regional long-section at 547000 mE

Figures 18–21 show representative plots of the model design, regional S_V pattern and two small-scale examples of the stress patterns associated with the southern and northern zone faults, respectively. Similar to the results for the regional cross-section, all three stress tensors (i.e. S_H, S_h and S_V) display stress perturbations along the fault planes of the shallow to moderate south- and north-dipping faults. These

stress patterns suggest that these faults are critically stressed faults and potentially zones of enhanced permeability (Figures 20 and 21). These anomalies are not observed with sub-horizontal faults. Again, this pattern is expected under the imposed thrust fault stress conditions and its relatively high magnitude of E–W oriented compression (S_H).

5. Conclusions

The current lack of local *in situ* stress measurements at the Charleton-Lemont project is a source of some technical uncertainty. However, the ~E–W oriented thrust fault stress regime interpreted from the recent and proximal Midlands earthquake event is broadly supported by other regional datasets. Although this information has provided only one local data point, if correct, earthquake data can provide reliable indicators of the 'far-field' stress regime and its orientation. The apparent thrust fault stress regime for this region is optimal for EGS developments as hydraulic stimulation is expected to result in approximately horizontal fracture/reservoir growth. An ~E–W maximum horizontal stress (S_H) orientation indicates that 'critically stressed' fractures/faults would be either steeply dipping, ~NE–SE trending structures or shallow (<45°) dipping structures such as shallow thrust and back splay faults observed in the regional cross- and long-sections. Estimates of local stress magnitude data are more uncertain, however, all datasets reviewed broadly correspond to a differential stress regime (i.e. S_H, S_h and S_V) of approximately 2 : 1.5 : 1.

An analysis of the modelling results for both the regional cross- and long-section indicate that shallow to moderate dipping faults are potentially critically stressed. This result correlates with that predicted by the theory of stress-dependent fracture permeability. Without direct drill testing it is impossible to know the exact nature and stress state of these particular fault structures, however, based on these modelling results they should be viewed as favourable Fault Play targets.

Both versions of the 5000 m depth horizontal planar models contained two fault intersections that appear to be critically stressed and potentially zones of enhanced permeability. These two sites involve the intersection of ~N–S and ~NW–SE faults

hosted within metasediments in close proximity to a granite contact. Of those two sites the southern fault intersection appears to have a more prominent stress field anomaly and should rank higher as a potential permeable fault intersection target (see Figures 10 and 13). If the inferred ~ENE-WSW trending fault in the 5000 m depth version 2 model is present then the stress anomaly associated with the southern site appears to be accentuated.

The model results of both versions of the 2000 m depth horizontal planar models indicated little to no stress field anomalies that might suggest any of the faults have reached a state of being critically stressed.

6. Key Assumptions & Limitations

These models are designed to assist explorers in areas of unknown or complex geology prior to drilling, however, large model parameter uncertainties means that the results are preliminary indications only i.e. a 'probabilistic' representation of potential fault stress states.

This work is based on geological interpretations and stress field data provided by KEN that have not been reviewed by HDR as part of this study. Furthermore, the hydrogeological and geomechanical properties of all rock units and faults at depth remain untested. The results of the numerical models are only as accurate as the input data. The quality of stochastic rock mass models is wholly dependent on the quality of the raw input datasets.

The results of modelling stated within this report have been generated using the best available estimates of critical parameters, but future work may yield new information that modifies or falsifies some of these assumptions. All modelling results should be treated as provisional.

7. References

ANDERSON, E.M., 1951, THE DYNAMICS OF FAULTING AND DYKE FORMATION WITH APPLICATION TO BRITAIN, EDINBURGH, OLIVER AND BOYD.

GENTIER, S., HOPKINS, D., AND RISS, J., 2000, ROLE OF FRACTURE GEOMETRY IN THE EVOLUTION OF FLOW PATHS UNDER STRESS. IN B. FAYBISHENKO, P.A. WITHERSPOON AND S.M BENSON (EDS) DYNAMICS OF FLUIDS IN FRACTURED ROCKS, WASHINGTON, D.C., AGU GEOPHYSICAL MONOGRAPH 122, 169–184.

GUDMUNDSSON, A., BERG, S.S, LYSLO, K.B. AND SKURTVEIT, E., 2001, FRACTURE NETWORKS AND FLUID TRANSPORT IN ACTIVE FAULT ZONES: JOURNAL OF STRUCTURAL GEOLOGY, 23, 343-353.

GUDMUNDSSON, A., SIMMENES, T.H., LARSEN, B. AND PHILIPP, S.L., 2009, EFFECTS OF INTERNAL STRUCTURE AND LOCAL STRESSES ON FRACTURE PROPAGATION, DEFLECTION AND ARREST IN FAULT ZONES: JOURNAL OF STRUCTURAL GEOLOGY, IN PRESS.

HILLIS, R. R., COBLENTZ, D. D., SANDIFORD, M., AND ZHOU, S., 1997, MODELLING THE CONTEMPORARY STRESS FIELD AND ITS IMPLICATIONS FOR HYDROCARBON EXPLORATION: EXPLORATION GEOPHYSICS, 28, 88–93.

HUDSON, J.A., STEPHANSSON, O., AND ANDERSSON, J., 2005, GUIDANCE ON NUMERICAL MODELLING OF THERMO-HYDRO-MECHANICAL COUPLED PROCESSES FOR PERFORMANCE ASSESSMENT OF RADIOACTIVE WASTE REPOSITORIES, INT. J. ROCK MECH. MIN. SCI. 42, 850–870.

MCCUE, K., VAN DISSEN, R., GIBSON, G. JENSEN, V AND BOREHAM, B., 2003. THE LAKE EDGAR FAULT: AN ACTIVE FAULT IN SOUTHWESTERN TASMANIA, AUSTRALIA, WITH REPEATED DISPLACEMENT IN THE QUATERNARY. ANNALS OF GEOPHYSICS 46(5), 1107–1117.

NELSON, E., HILLIS, R., SANDIFORD, M., REYNOLDS, S. AND MILDREN, S., 2006. PRESENT-DAY STATE-OF-STRESS OF SOUTHEAST AUSTRALIA. APPEA JOURNAL 46, 283–305.

SLOANE, D.J, 1991. SOME PHYSICAL PROPERTIES OF DOLERITE. TASMANIA DEPT. RESOURCES AND ENERGY, DIVISION OF MINES AND MINERAL RESOURCES, REPORT 1991/22.

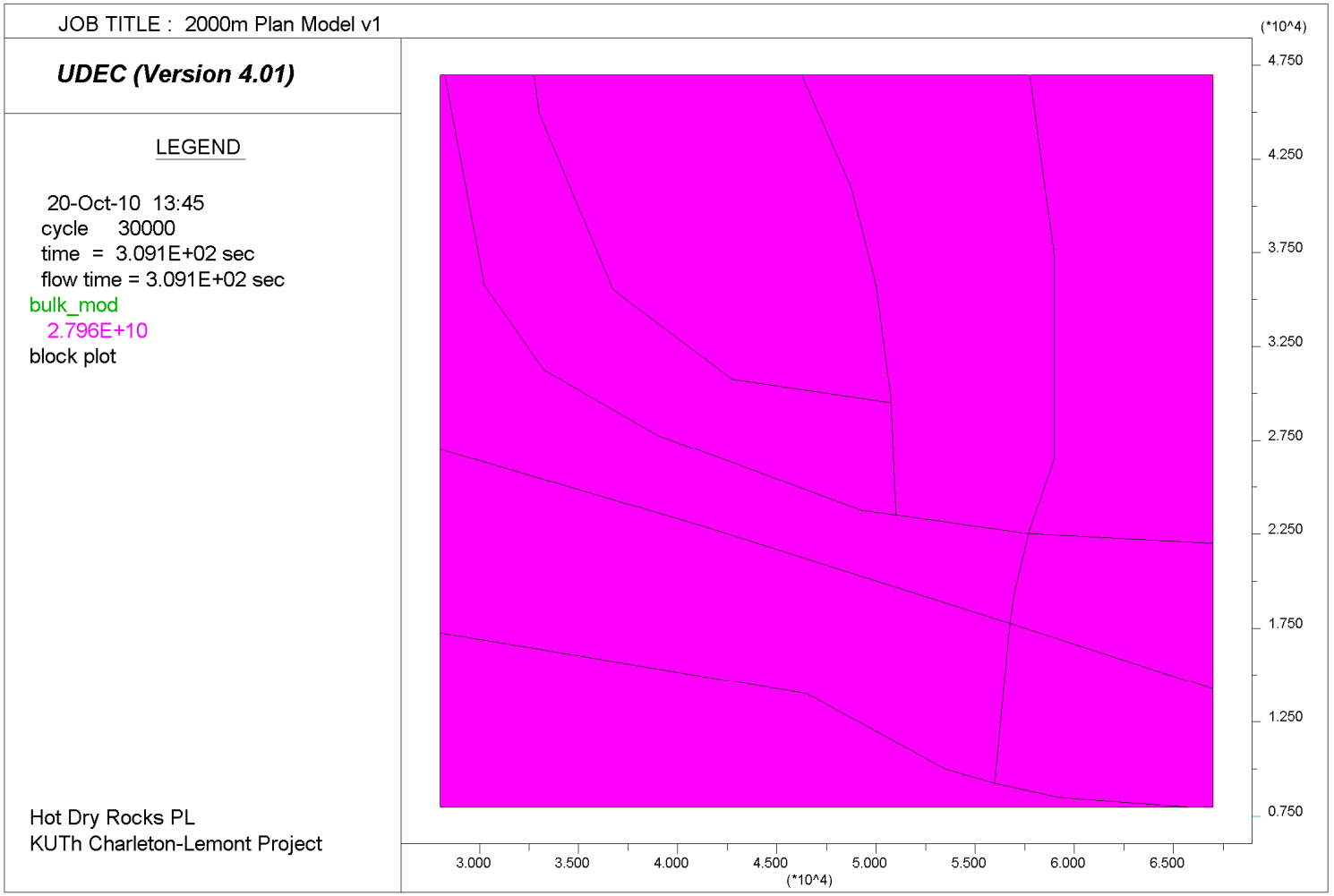

Figure 2. *Horizontal planar model at 2000m version 1: rock mass (pink=phyllite) plus fault structures (black).*

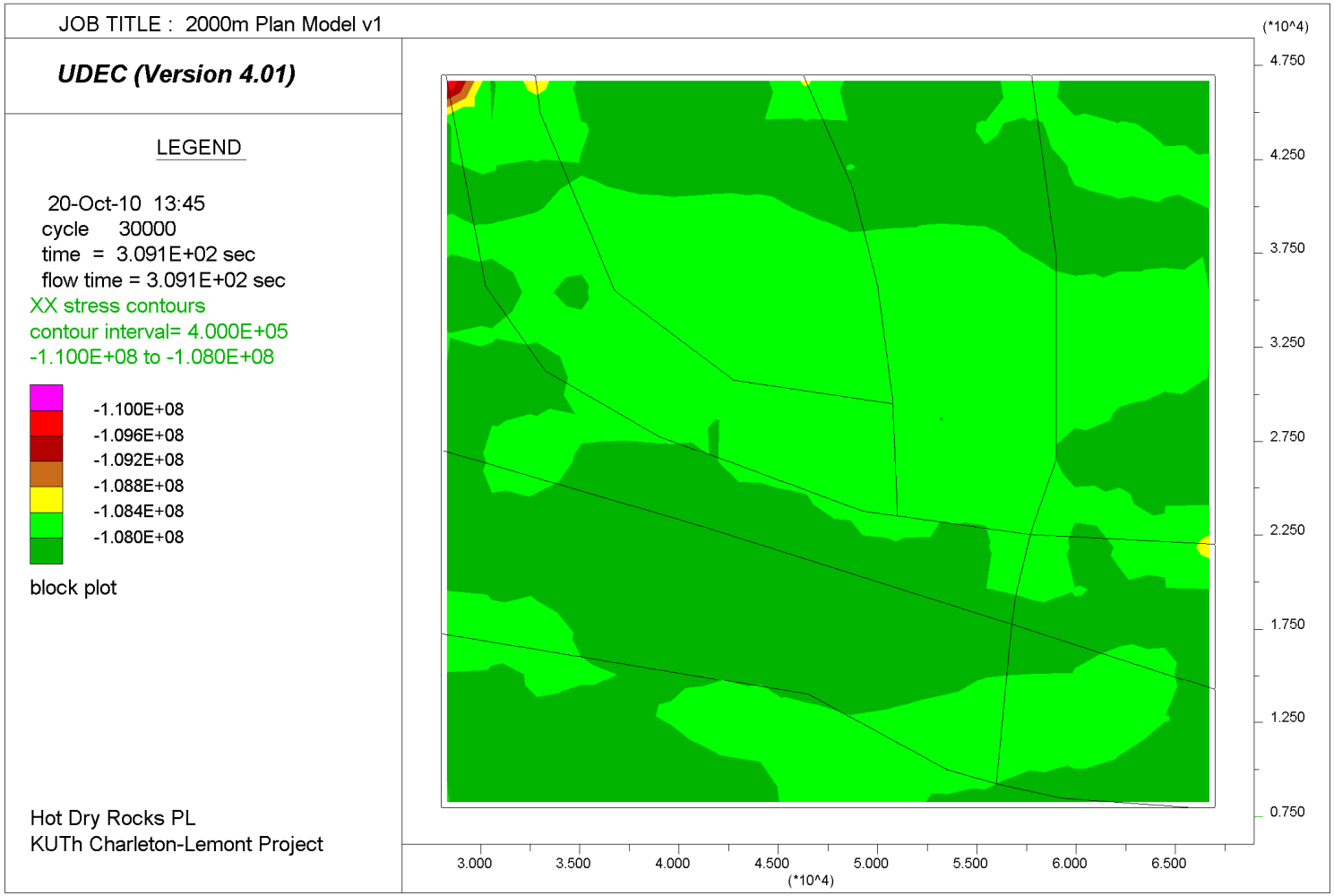

Figure 3. *Horizontal planar model at 2000m version 1: S_H (XX) stress contours. Negative contour values are compressive.*

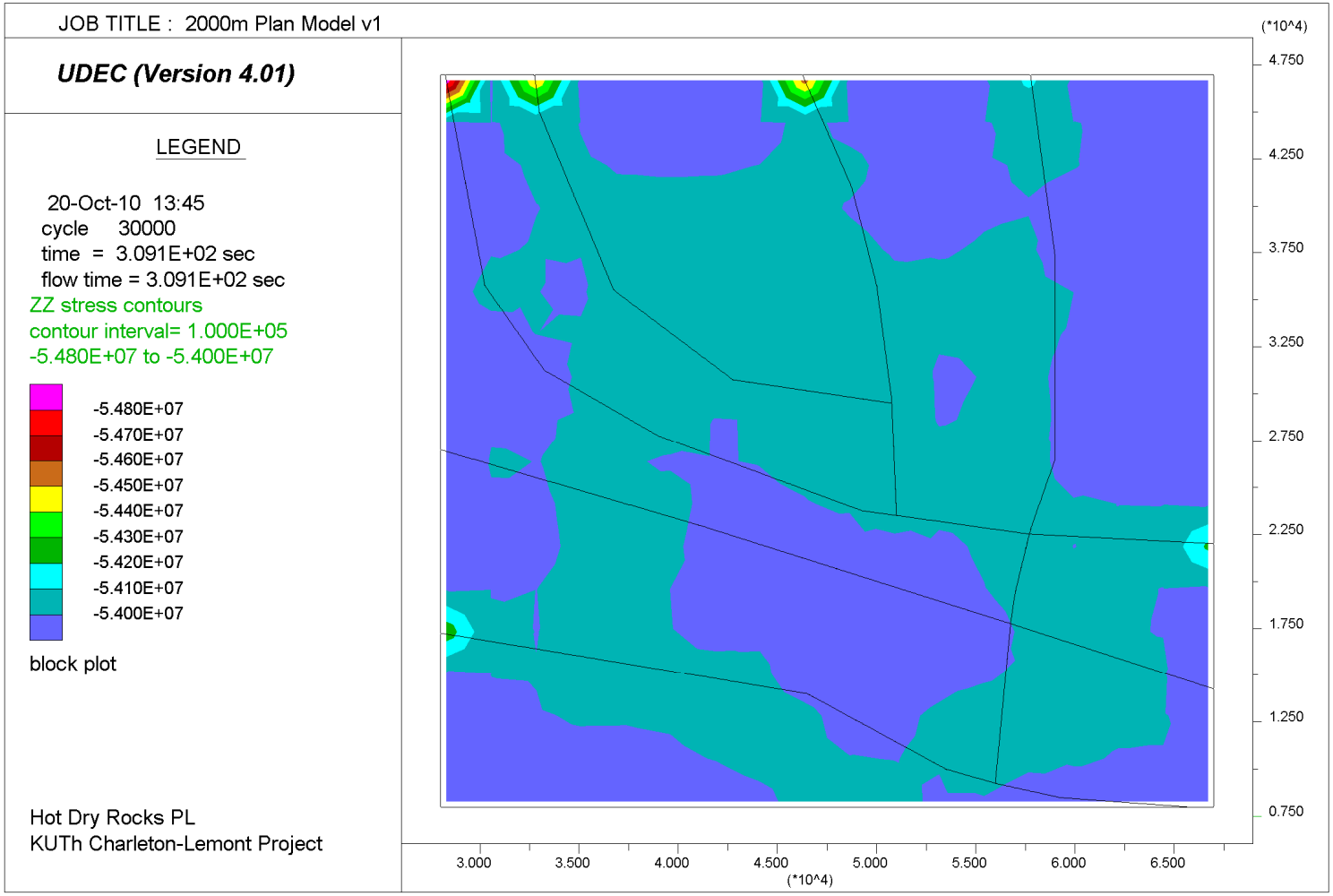

Figure 4. *Horizontal planar model at 2000m version 1: S_V (ZZ) stress contours. Negative contour values are compressive.*

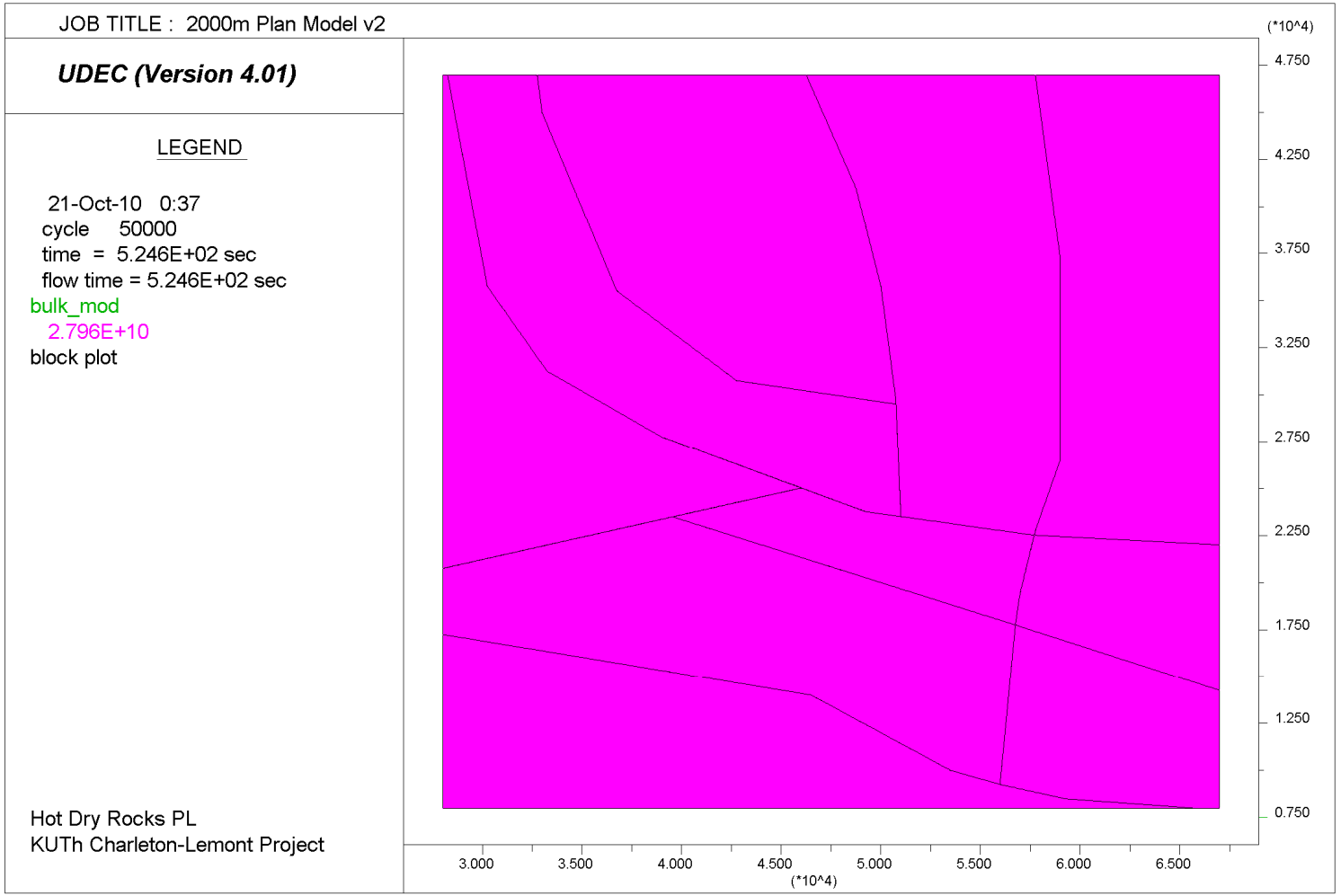

Figure 5. *Horizontal planar model at 2000m version 1: rock mass (pink = phyllite) plus fault structures (black).*

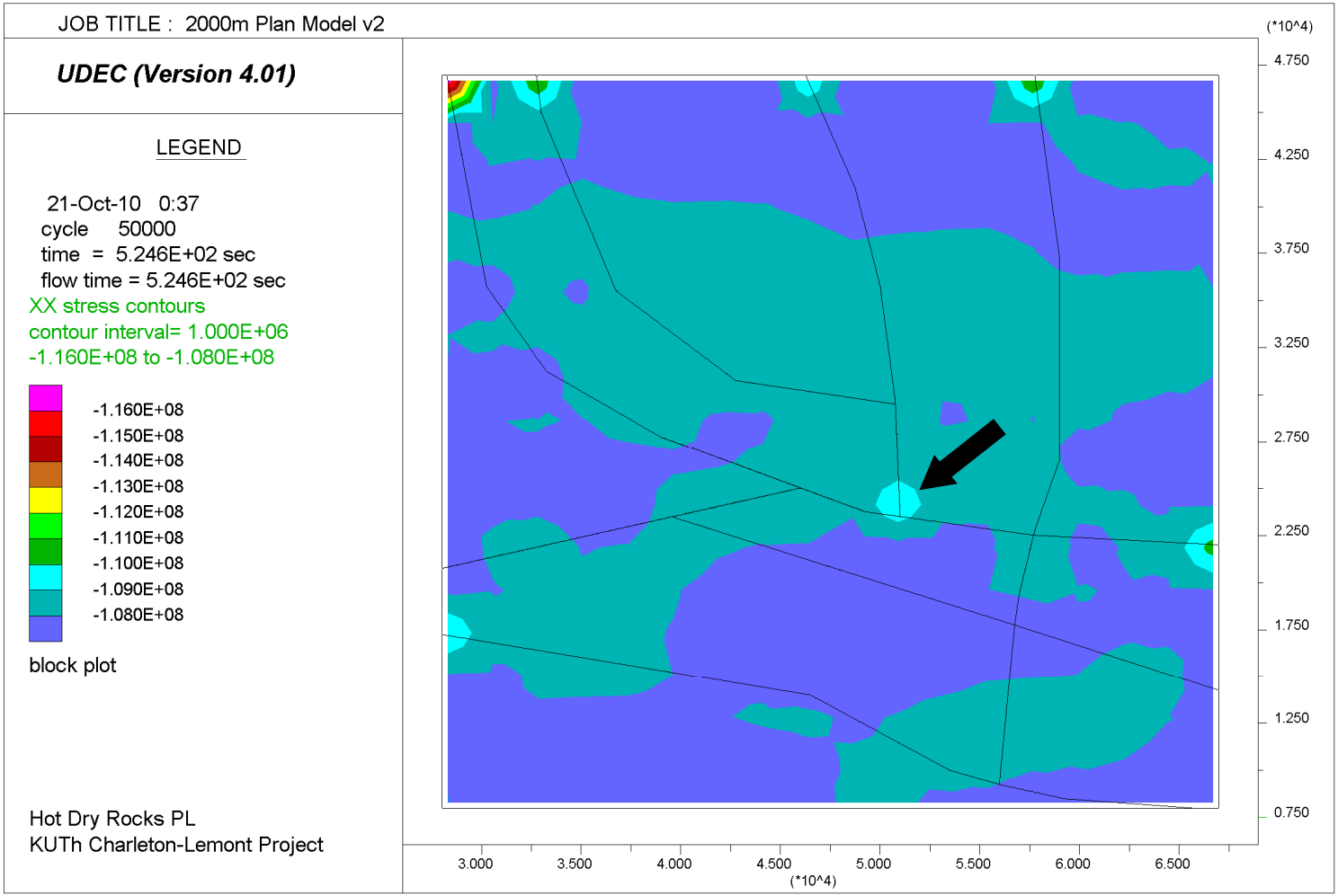

Figure 6. *Horizontal planar model at 2000m version 2: S_H (XX) stress contours. Note a subtle stress (low) anomaly at one fault intersection (highlighted by the black arrow). Negative contour values are compressive.*

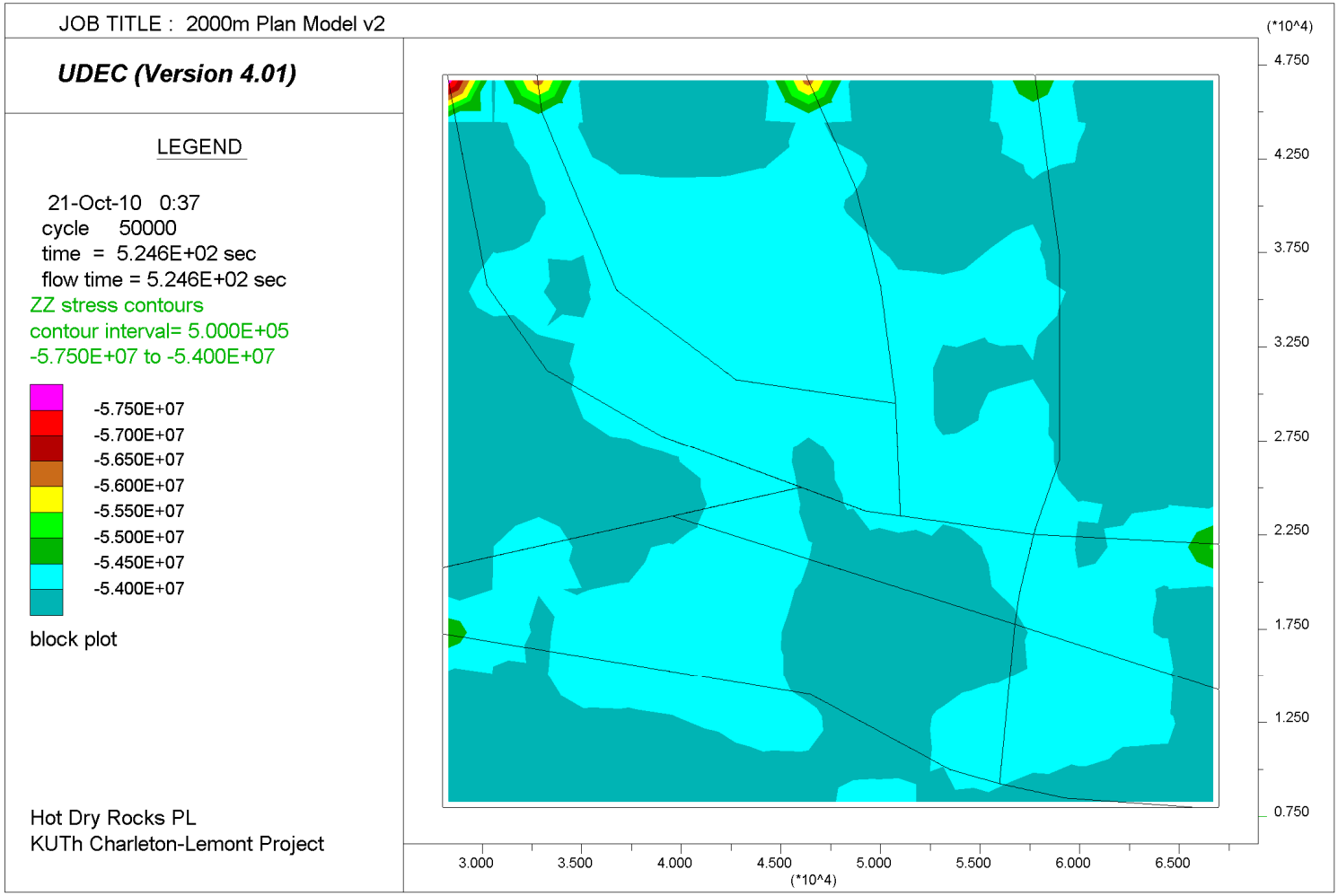

Figure 7. *Horizontal planar model at 2000m version 2: S_V (ZZ) stress contours. Negative contour values are compressive.*

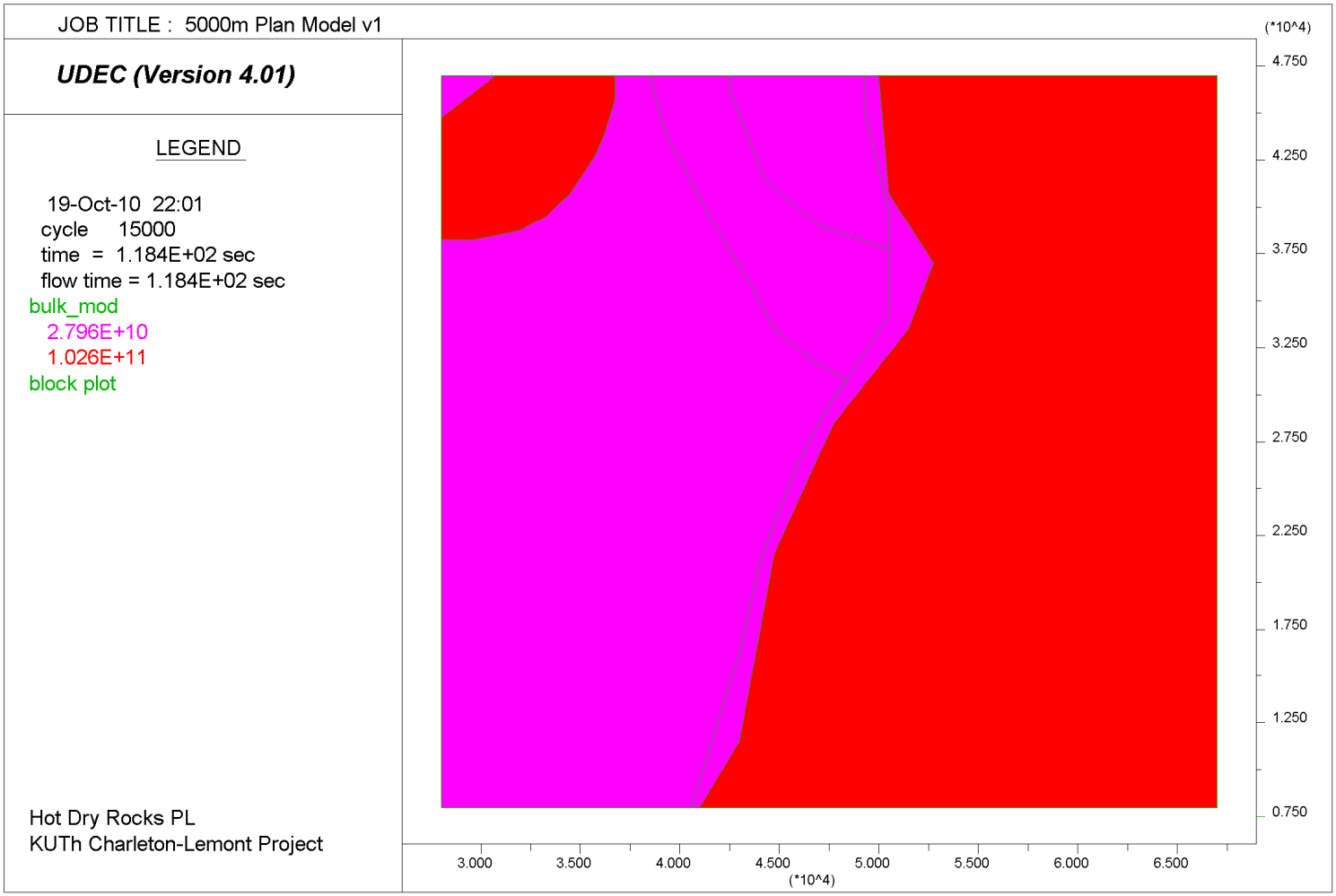

Figure 8. *Horizontal planar model at 5000m version 1: rock mass (pink=phyllite; red=granite) plus fault structures (black).*

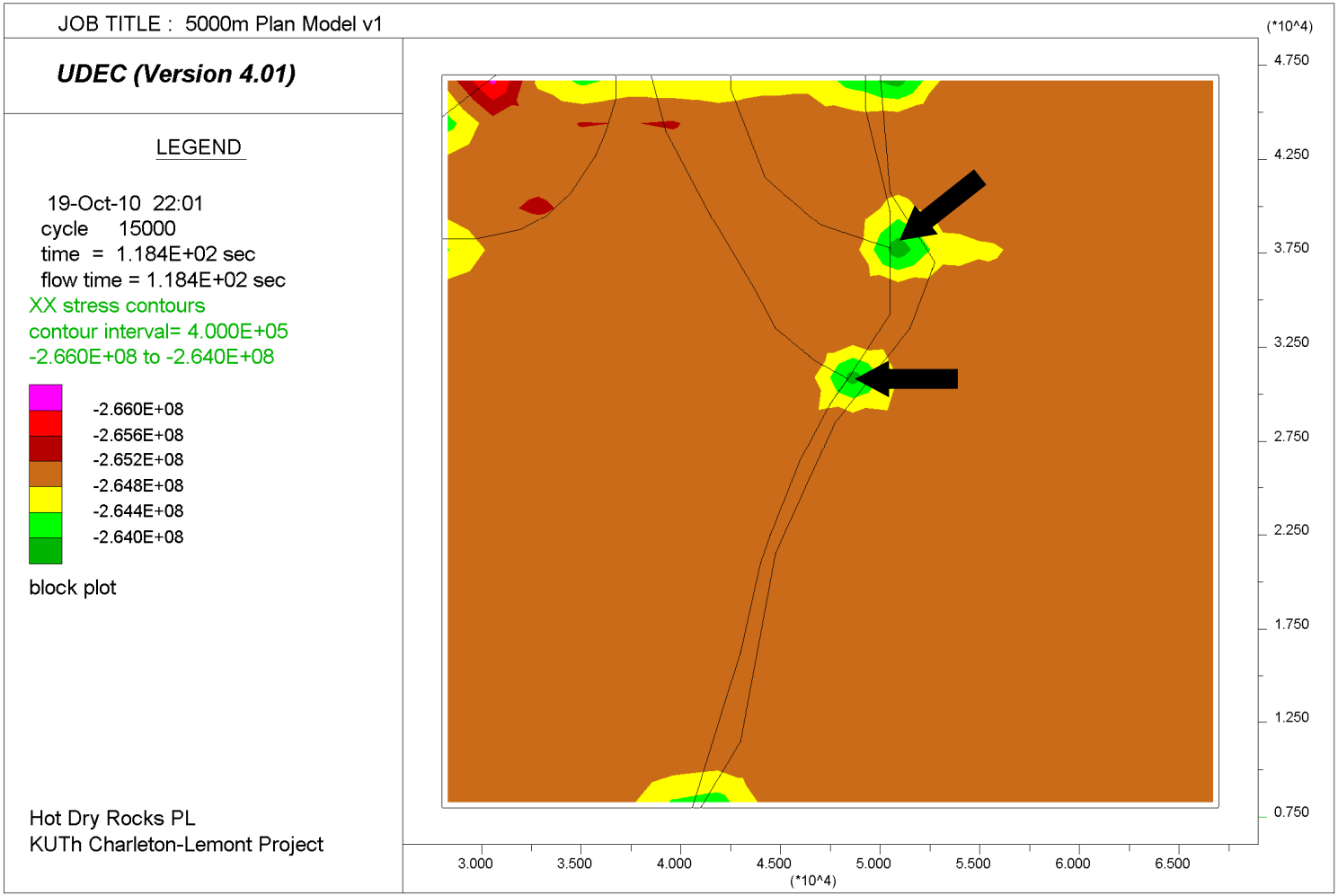

Figure 9. *Horizontal planar model at 5000m version 1: S_H (XX) stress contours. Note the obvious but subtle stress (low) anomalies located at two fault intersections (highlighted by the black arrows). Negative contour values are compressive.*

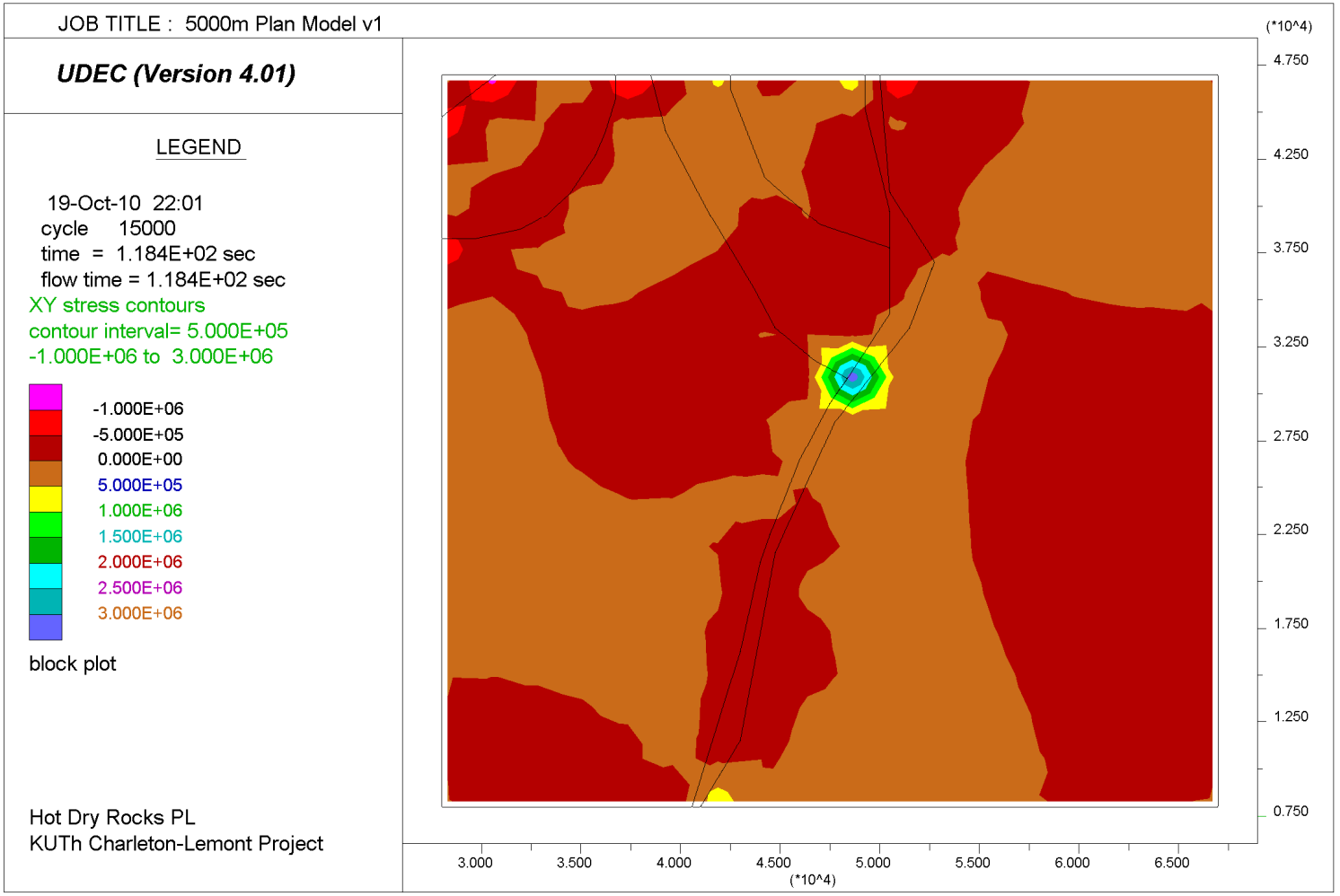

Figure 10. *Horizontal planar model at 5000m version 1: $S_{H,h}$ (XY) or horizontal shear stress contours. Note the obvious but subtle stress (low) anomalies located at the southern fault intersection of the two stress anomalies depicted in Figure 9. Negative contour values are compressive whilst positive values are tensional.*

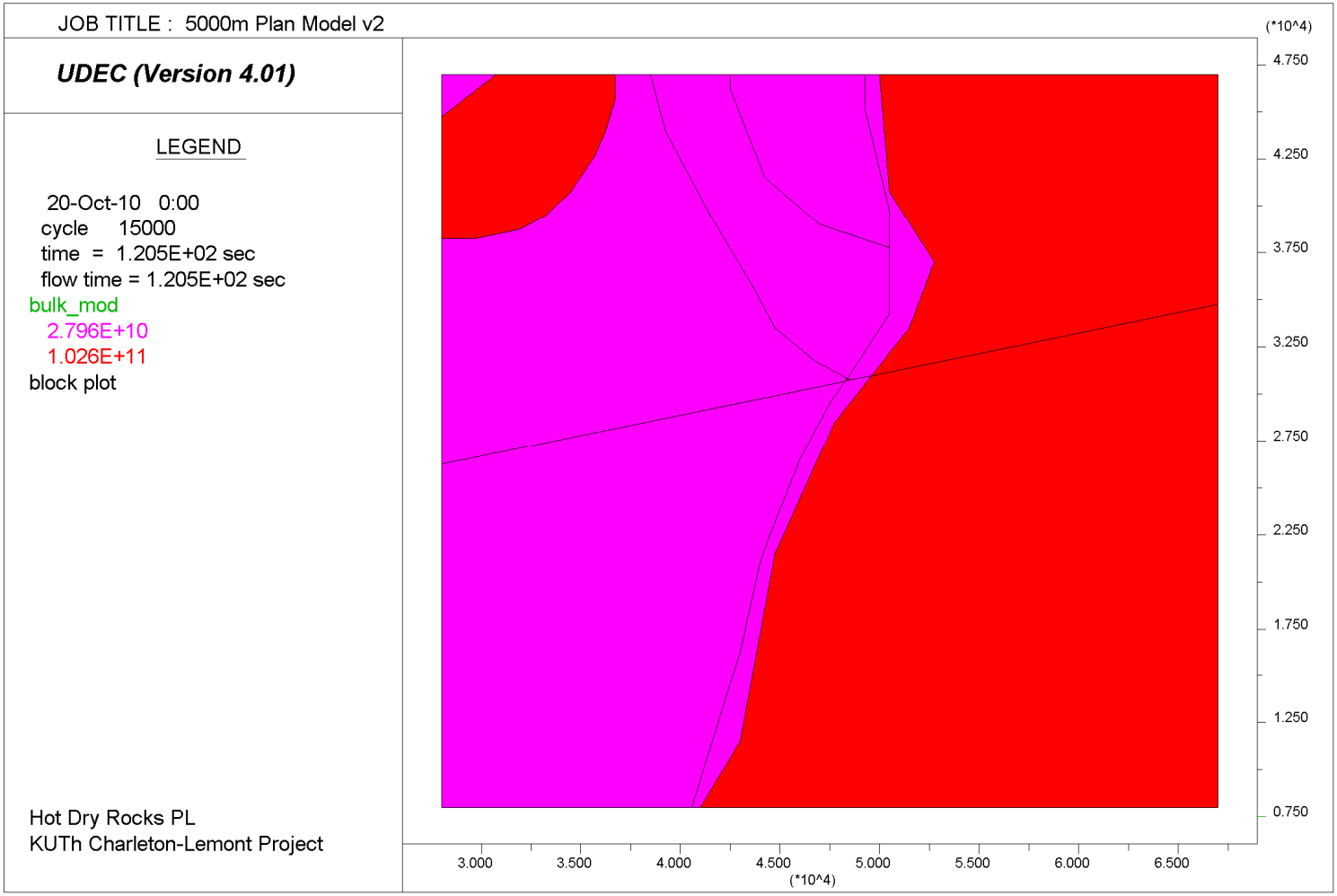

Figure 11. *Horizontal planar model at 5000m version 2: rock mass (pink=phyllite; red=granite) plus fault structures (black).*

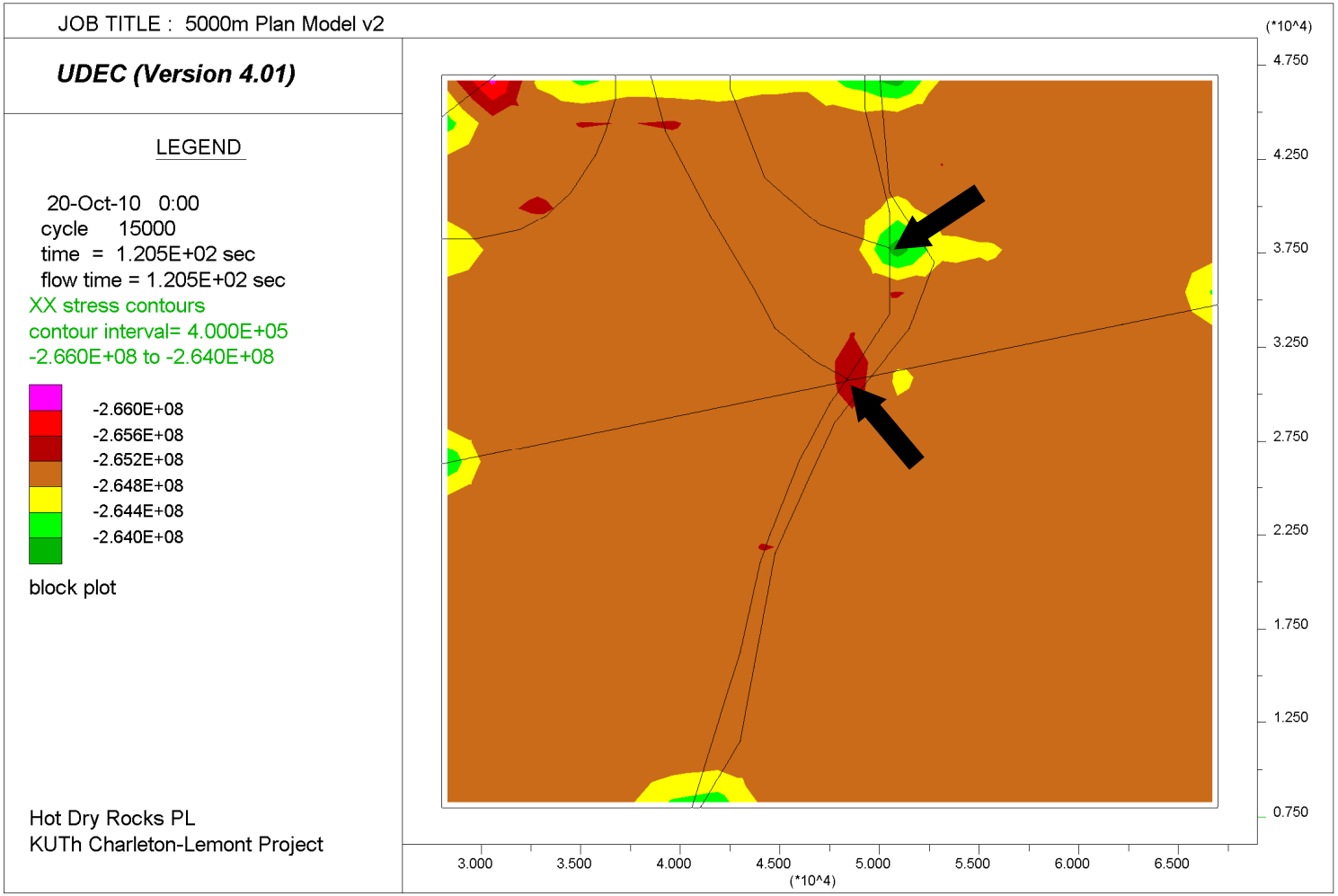

Figure 12. *Horizontal planar model at 5000m version 1: S_H (XX) stress contours. Note the obvious but subtle stress (low) anomalies located at two fault intersections (highlighted by the black arrows). Negative contour values are compressive.*

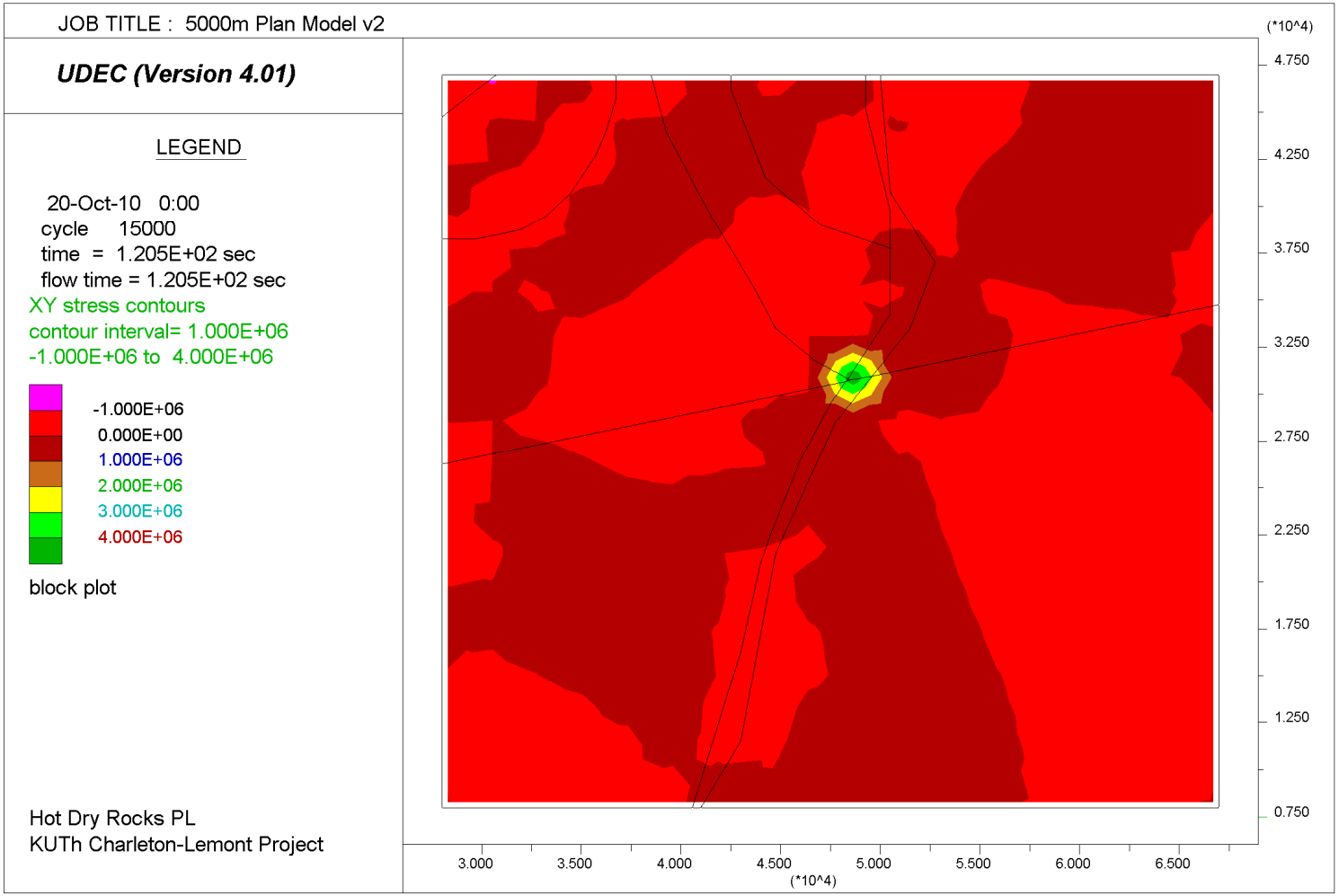

Figure 13. *Horizontal planar model at 5000m version 2: $S_{H,h}$ (XY) or horizontal shear stress contours. Note the obvious but subtle stress (low) anomalies located at the southern fault intersection of the two stress anomalies depicted in Figure 9. Negative contour values are compressive whilst positive values are tensional.*

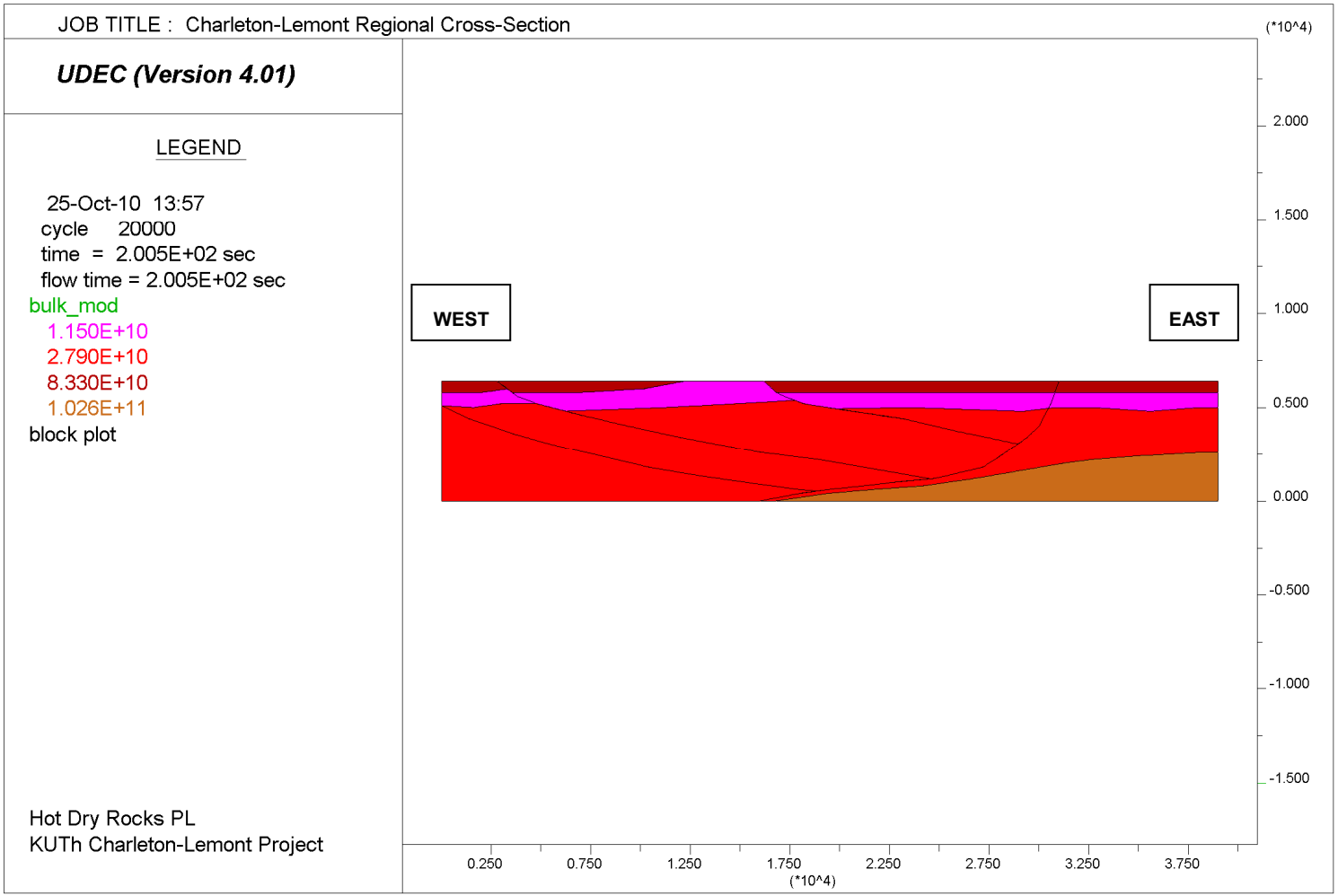

Figure 14. *Regional cross-section model: rock mass (dark brown=dolerite; pink=siltstone; red=phyllite; light brown=granite) plus fault structures (black).*

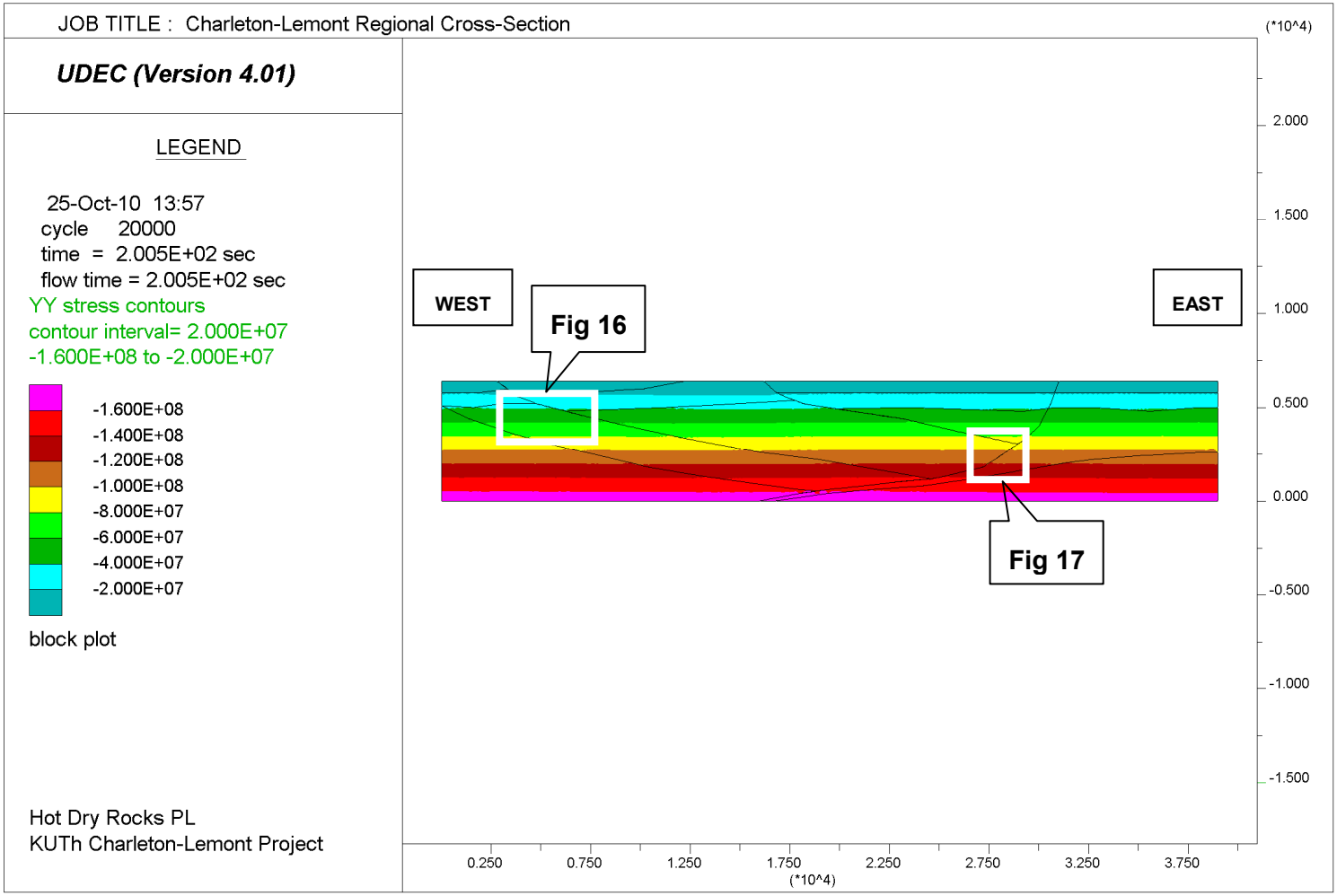

Figure 15. *Regional cross-section model: regional S_V (YY) stress contour pattern. Negative contour values are compressive.*

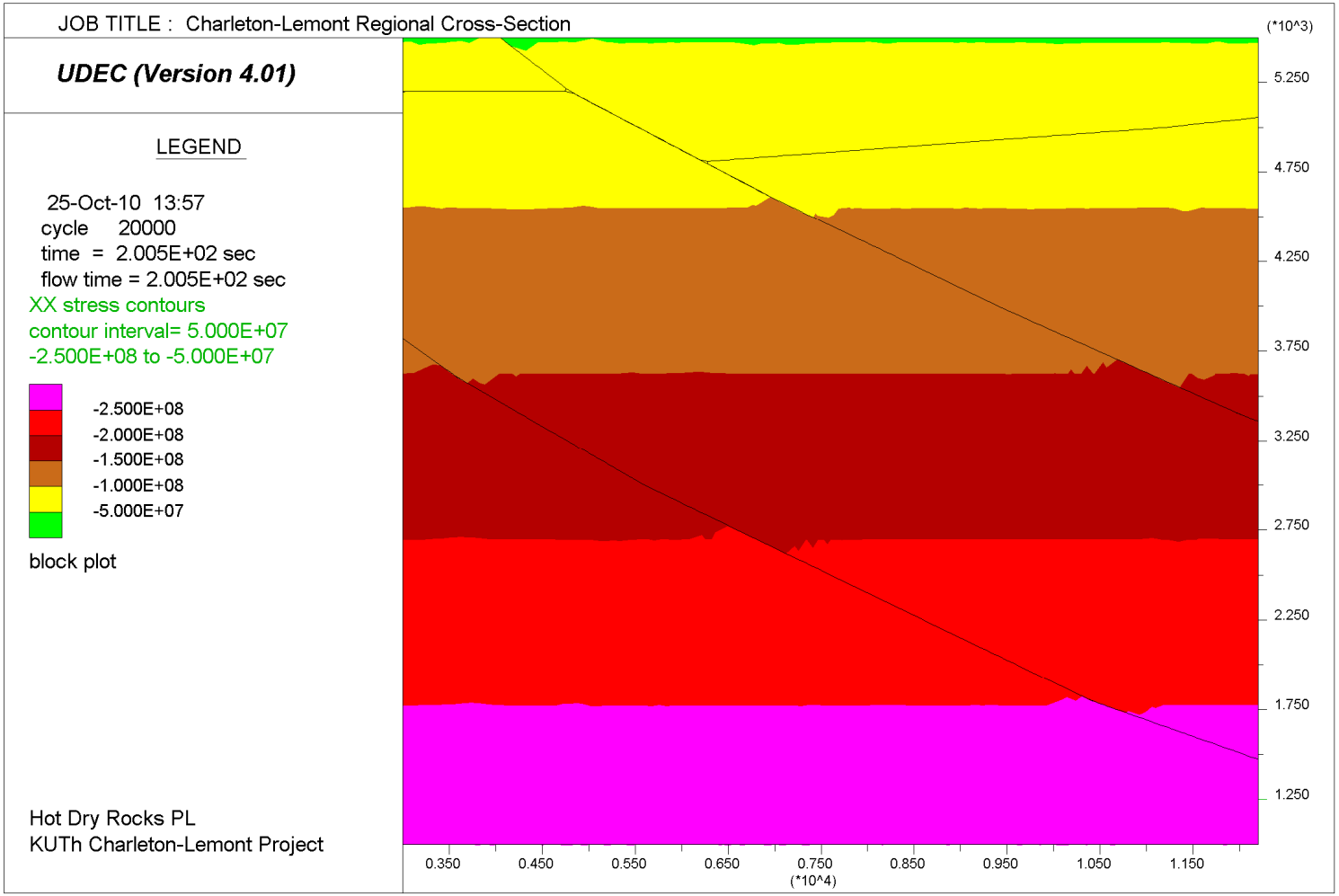

Figure 16. *Regional cross-section model – western zone faults: S_H (XX) stress contours. For location see inset Figure 15. Note the S_H stress perturbation pattern along the fault hangingwall (low) and footwall (high) of the shallow east-dipping faults. Negative contour values are compressive.*

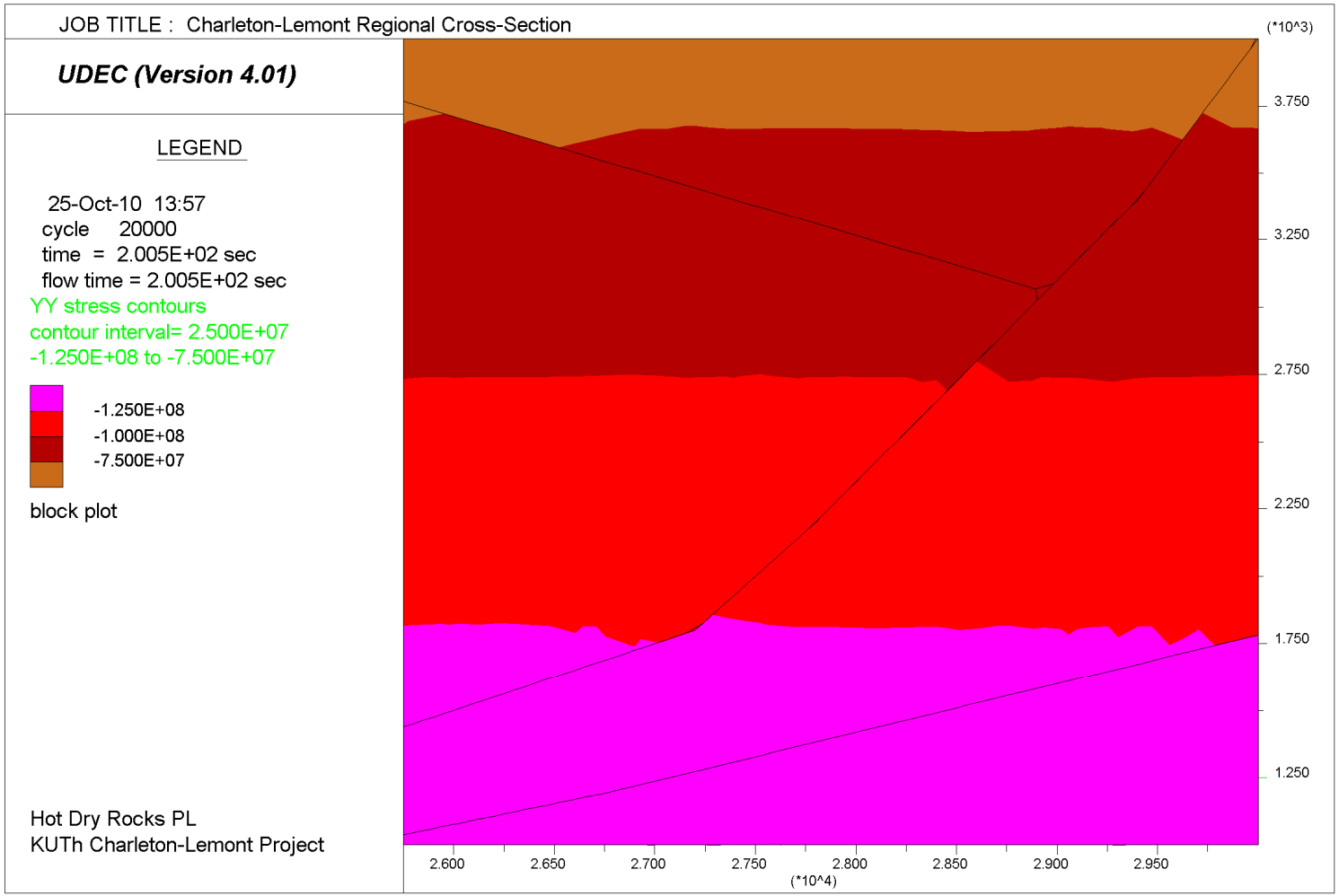

Figure 17. *Regional cross-section model – eastern zone faults: S_V (YY) stress contours. For location see inset Figure 15. Note the S_V stress perturbation pattern along the fault hangingwall (low) and footwall (high) of the moderate dipping faults. Negative contour values are compressive.*

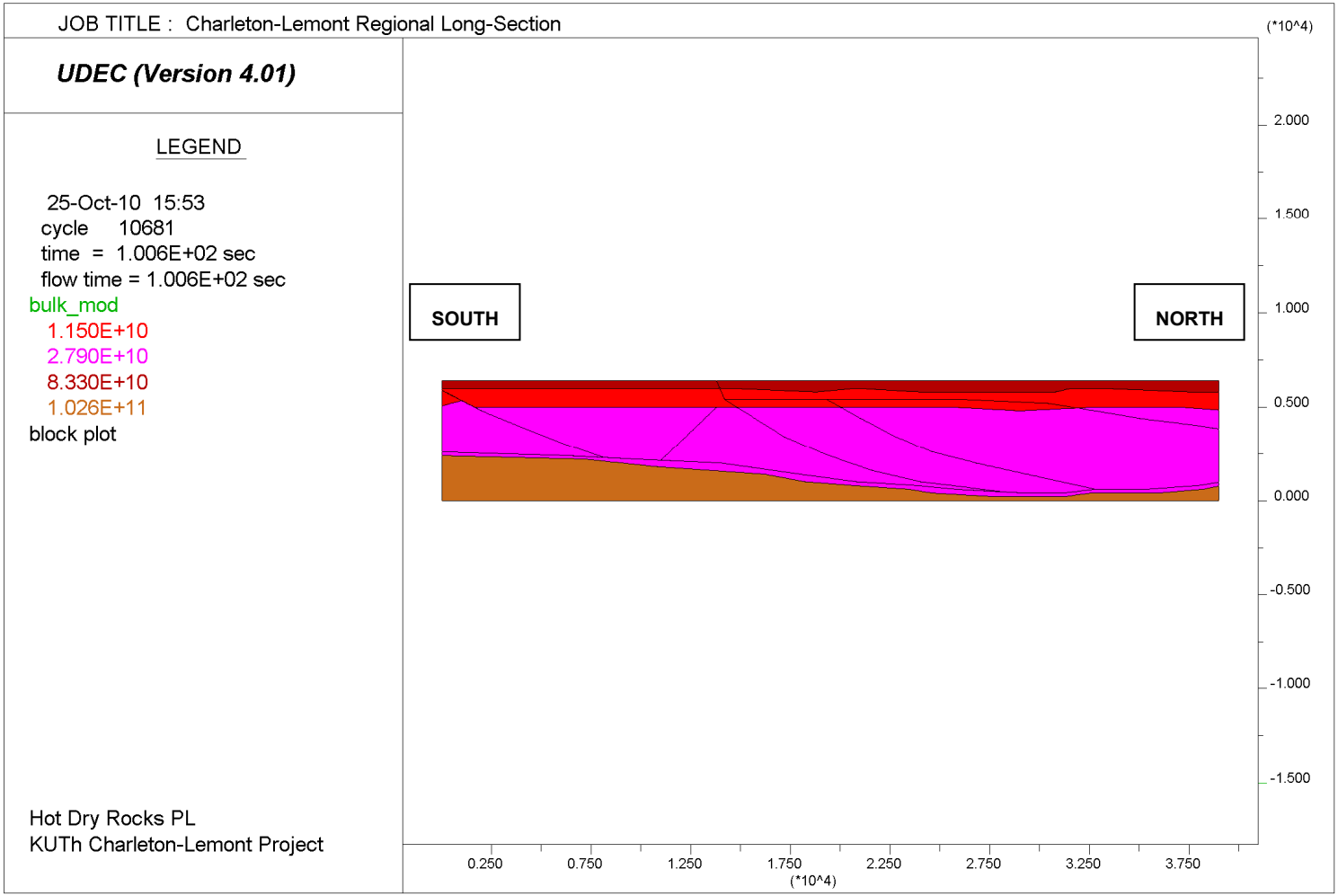

Figure 18. *Regional long-section model: rock mass (dark brown=dolerite; red=siltstone; pink=phyllite; light brown=granite) plus fault structures (black).*

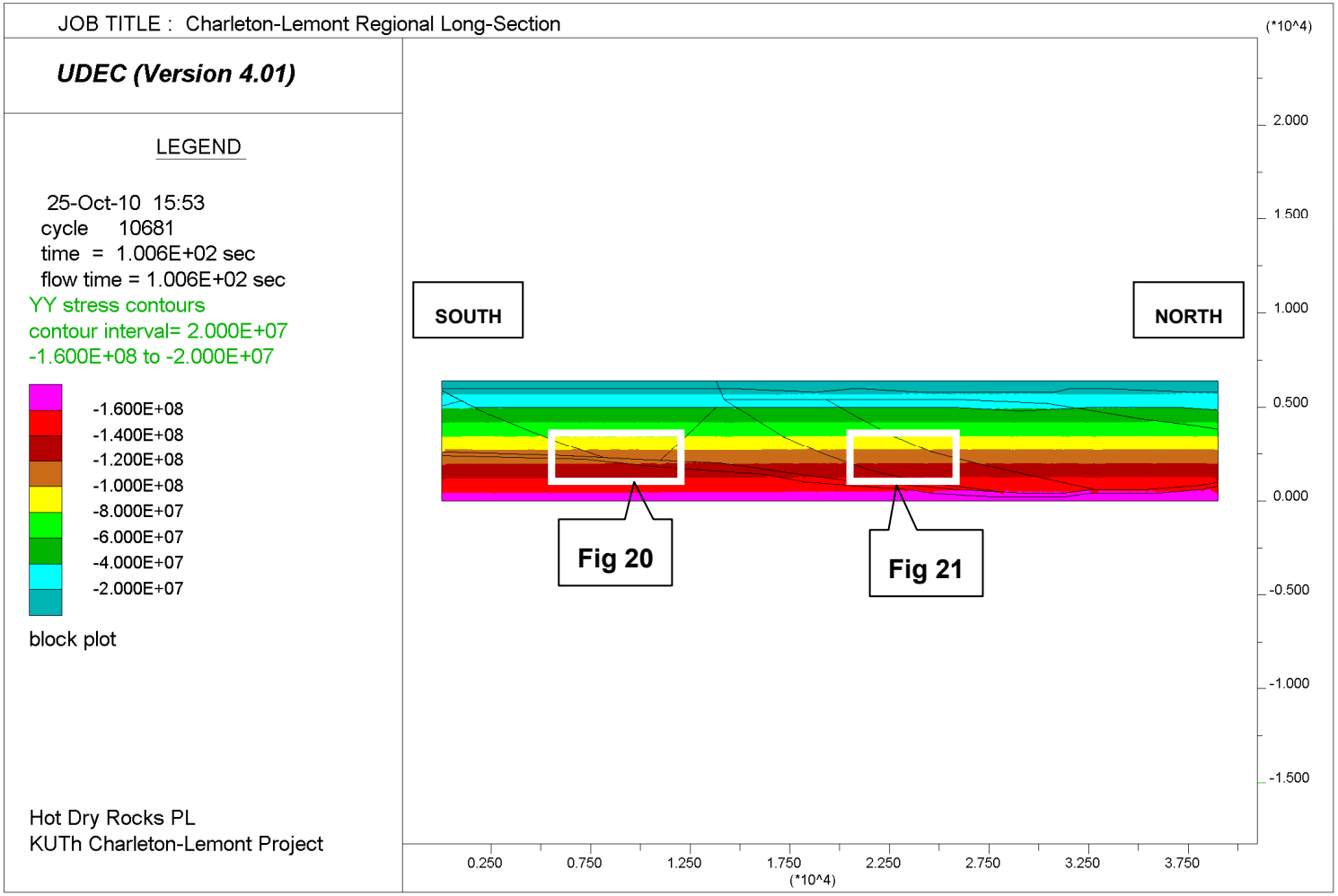

Figure 19. *Regional cross-section model: regional S_V (YY) stress contour pattern. Negative contour values are compressive.*

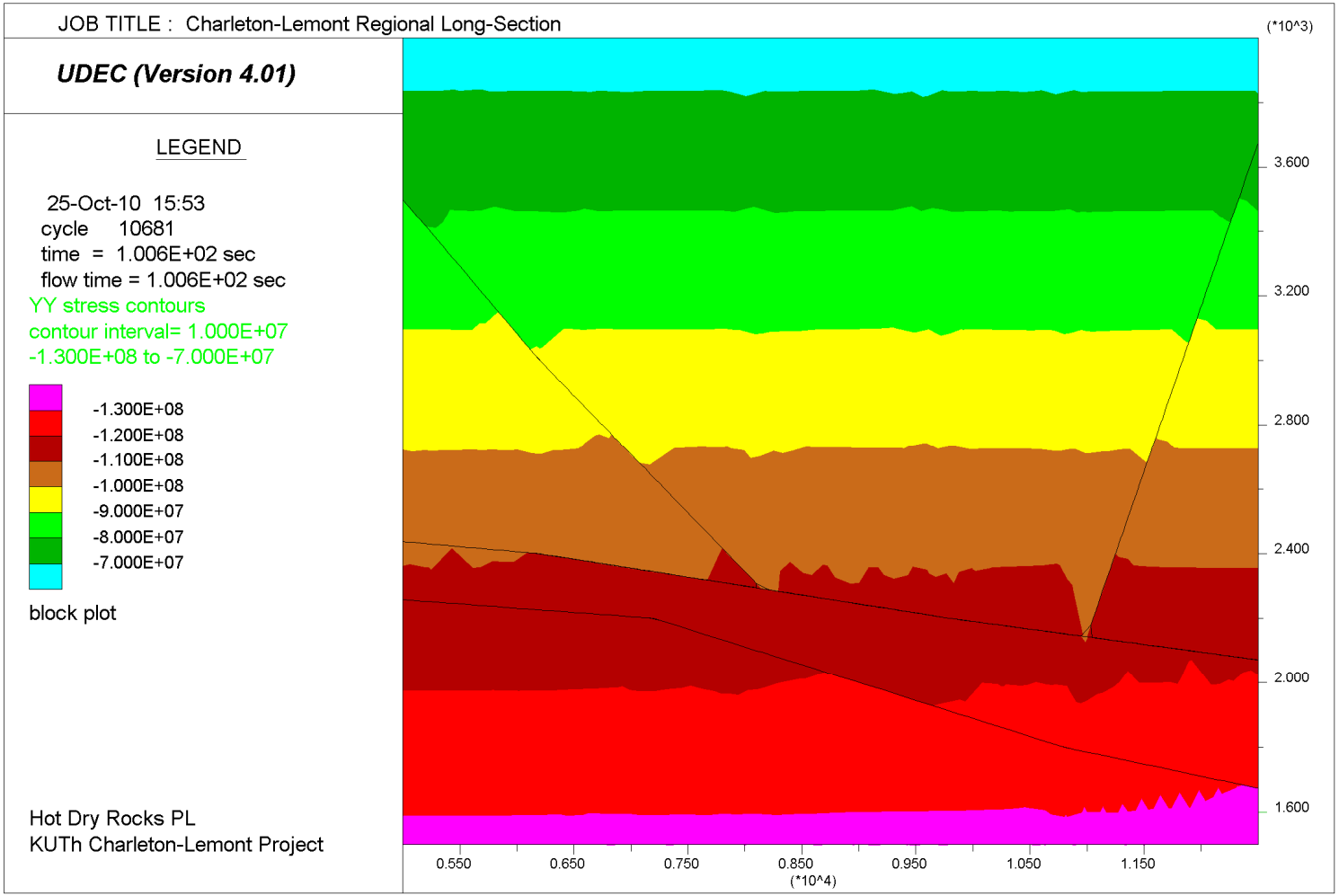

Figure 20. *Regional cross-section model – southern zone faults: S_V (YY) stress contours. For location see inset Figure 19. Note the S_V stress perturbation pattern along the hangingwall (low) and footwall (high) of the shallow and moderate dipping faults. Negative contour values are compressive.*

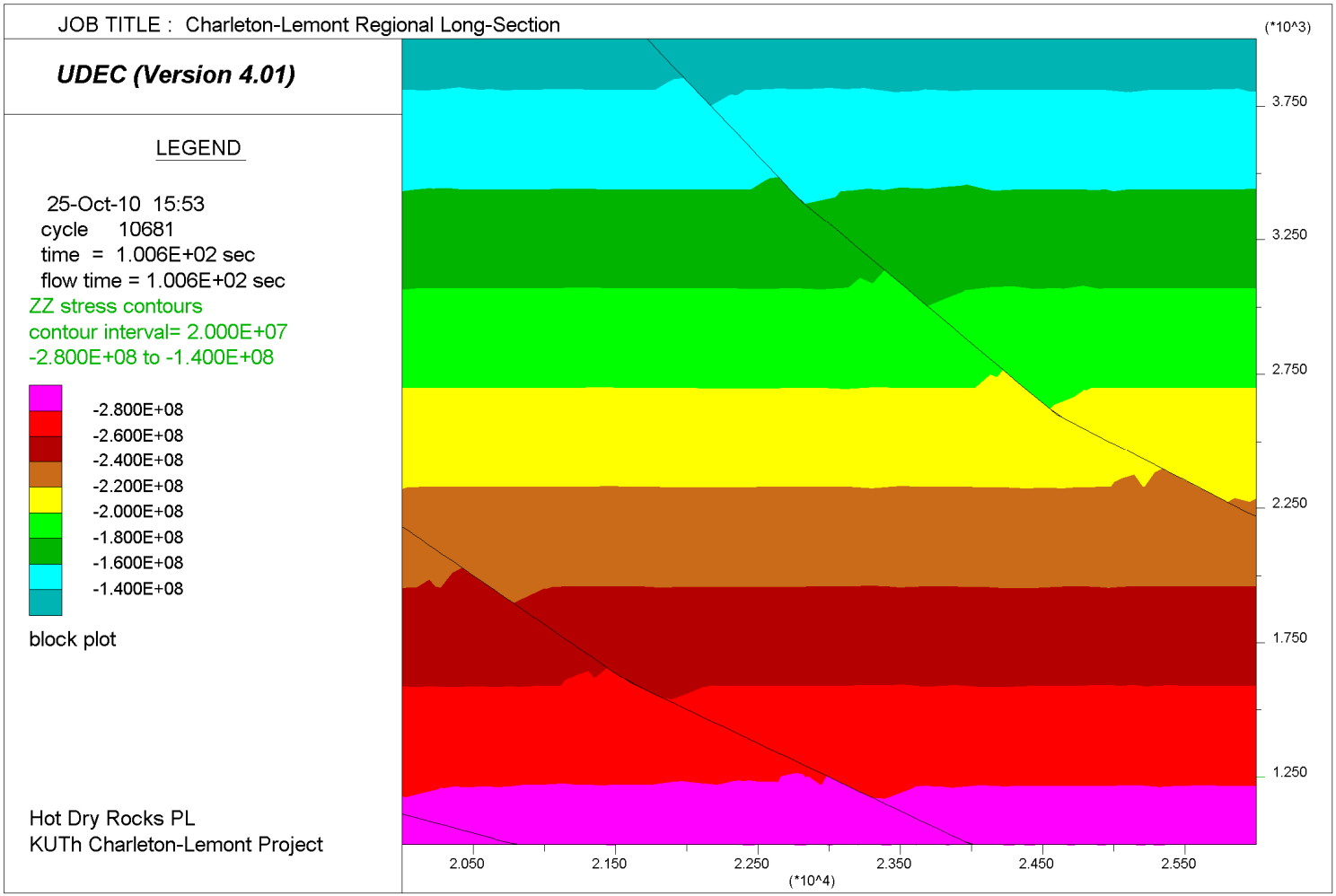

Figure 21. *Regional cross-section model – northern zone faults: S_H (ZZ) stress contours. For location see inset Figure 19. Note the S_H stress perturbation pattern along the hangingwall (low) and footwall (high) of the shallow–moderate dipping faults. Negative contour values are compressive.*